DESY, Hamburg, Germany
IHEP, Protvino, Russia

Accelerator Physics Seminar, January 28, 2003

Noise Performance Studies at the HERA-*p* Ring

S. Ivanov and O. Lebedev

Attachment #88 (April 2002)
to the Agreement between DESY, Hamburg and IHEP, Protvino

Contents

1 Preamble: Motivations

Beam observations + coasting-beam halo effect in the HERA-*p*

⇓

Noises in RF system (or ripple in *B*-field) could be responsible for longitudinal beam degrade

Many various **PARAMETERS** are tied together simultaneously. To list a few:

Life-times

1. Transverse exponential — $\tau_t \cong 100$ hr
2. Instantaneous initial σ_φ-doubling — $\tau_{\sigma 2} \cong 10$ hr
3. Instantaneous initial emittance ($\bar{J}$-) doubling — $\tau_{J2} \cong 5$ hr for $\bar{J} \propto \sigma_\varphi^2$

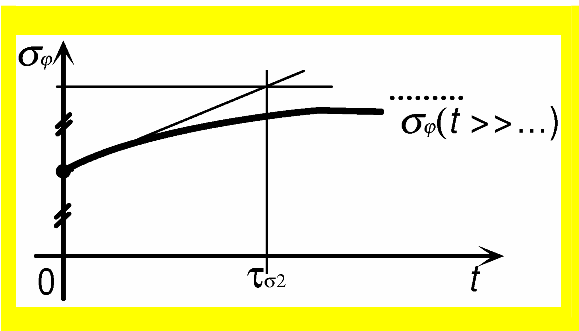

To note:

Parameter $\tau_{J2} \propto \sigma_\varphi^2(t = 0)$

Above figures apply to injected bunch occupying ½ of RF bucket at foot of distribution

Asymptotic length of a bunch

FWHM = 1.8–1.9 ns @ t > 10–22 hr (i.e., @ $t \to \infty$)

Loss rate of bunched-core population

5–10 % away after 10 hr

SR of high-energy protons

9.5 eV/turn @ 920 GeV (over-voltage factor of about 10^5)

6.0 eV/turn @ 820 GeV

Momentum acceptance

$$\Delta p/p_0 \cong \pm(1\text{–}5)\cdot 10^{-3}$$

Coasting-Beam halo

p-DC minus *p*-bunched currents

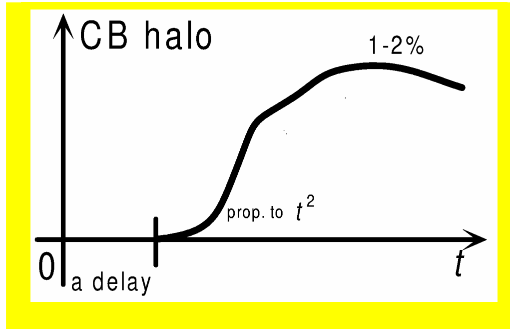

Role of composite 2 RF bunches

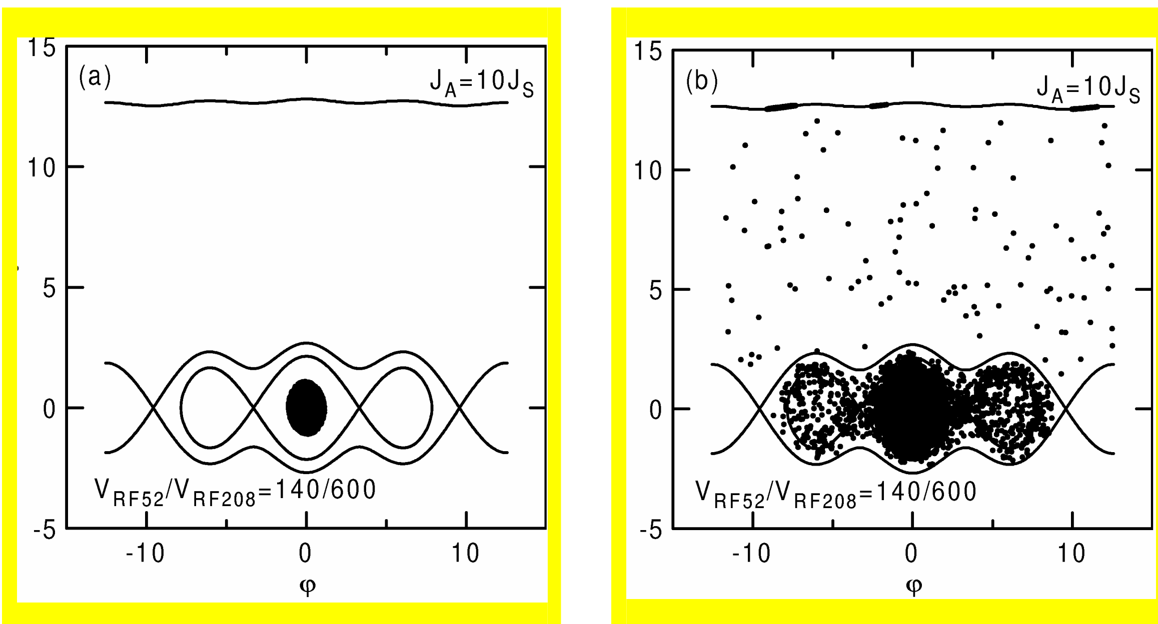

- Phase/frequency noise of RF system is, normally, the 1st to show itself up.
- The 208 MHz potential well is steeper (and more **non-linear**!) than that of 52 MHz.

These were the motivations to launch Attachment #88 to the IHEP-DESY Agreement, Re:

Noise Performance Studies at the HERA-*p* Ring

2 Strategy

Priority order:

208 MHz → 52 MHz → forced beam response → *B*-field ripple

Goals of the study:

1. Detect the presence of noise,
2. Spot the noisy sub-system,
3. Reveal the nature of noise, and
4. Start elaborating adequate cures.

Boundary conditions:

1. Non-intervening diagnostics, in the sustained run-2002 of the machine.
2. Save time and investment cost → use of equipment, components and signals already available in the HERA-*p* instrumentation.

Underlying technique — analog *I*/*Q* demodulation about the 208 & 52 MHz references. A double-purpose tool:

1. To measure noises in cavity voltages.
2. To diagnose forced beam response to noise at coupled-bunch mode $m = 1, 2$ and $n = 0$.

Courtesy of E. Vogel — head part of his tool for [fast] cavity and beam diagnostics system.

3 Time Schedule

Three series of measurements accomplished in run-2002 of the HERA-*p*.

First, June 2002

What is found:

1. Heavy stray fields in bld. 50/room 601 precluding straightforward diagnostics. Say, programmable filter KH-3901 by the Krohn-Hite Corp. failed to operate in the actual environment.
2. Technically, phase of the LO could not be locked to phase of an RF cavity.
3. Digital scope TEKTRONIX TDS 684A could not yield power-spectrum processing even for diagonal *II* & *QQ* spectra.

Decisions taken in the aftermath:

1. To manufacture a dedicated high-gain low-noise base-band AC-coupled shielded differential 2-channel amplifier. ☑
2. To develop an off-line post-processing code with a capability of cross-correlation analysis and data rotation to the gap frame. ☑

Then, September 2002

What is found and done:

1. Live test of subtraction (differential) technique with the purpose-built amplifier (gain = 300, bandwidth = 5 Hz – 1.1 kHz).
2. In-the-field test of data post-processing procedure.
3. Unsettled close-to-DC behavior of the issued DC-coupled low-pass amplifiers at the final ends of *I*/*Q* demodulation units (gain 2–5, cut-off 2 kHz @–3 dB). It was by-passed. (Side effect — shortening signal transport path unattended with the subtraction technique).
4. Attained resolution flat-bottom of power spectrum detection at about a few units of $10^{-13}\ 1^2$/Hz.
5. Better than expected noise conduct of 208 MHz cavities (A, B, C, and D).
6. Higher noise in 52 MHz cavities (A, B)? It was yet an uncertain outcome of measurements.

Decisions taken in the aftermath:

1. To settle the stuff for further studies, off-line @ IHEP. ☑

And, finally, December 2002

What is found and done:

1. Lasting routine measurements in smooth operational conditions.
2. Priority order turned around. First, 52 then 208 MHz cavities.
3. Album compiled of representative data plots for each of 4+2 RF cavities installed.
4. Seems to have found the most challenging cavity, namely, the B 52 MHz.
5. Beam response measurements via resistive gap monitor signal in a 52 MHz band. Mostly, as the effect tracer @ coupled bunch mode m =1 and n = 0.

4 Principles of DA and Analysis

4.1 I/Q Decomposition

Accelerating field above transition

$$-V_{RF}\cdot\sin(\omega_{RF}t) \text{ across an equivalent gap}$$

I/*Q* rotating Cartesian basis:

	Gap frame	LO frame
In-phase	$-u_I(t)\cdot\sin(\omega_{RF}t)$	$-u_I(t)\cdot\sin(\omega_{RF}t-\phi)$
Quadrature	$-u_Q(t)\cdot\cos(\omega_{RF}t)$	$-u_Q(t)\cdot\cos(\omega_{RF}t-\phi)$

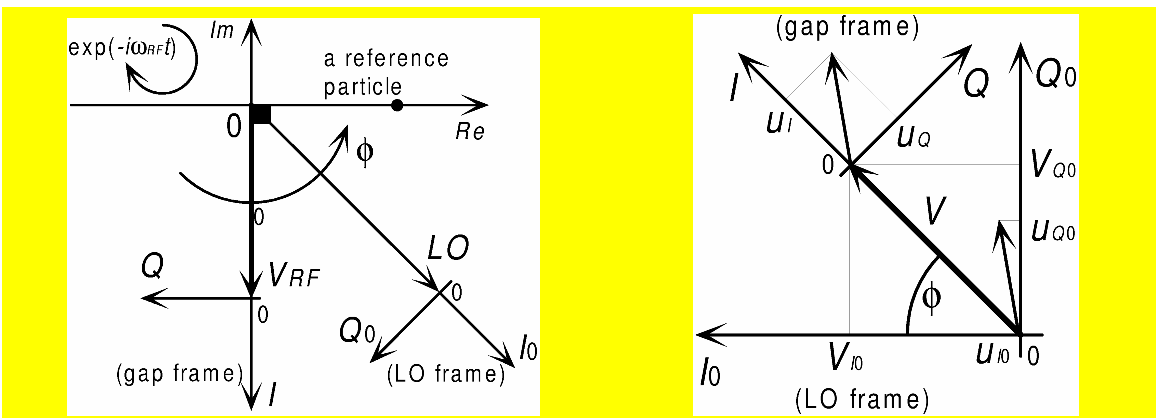

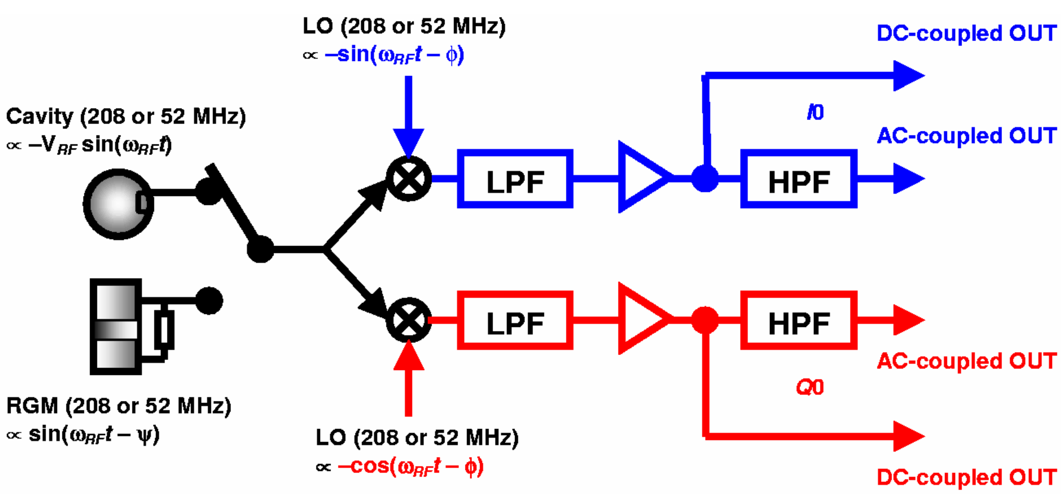

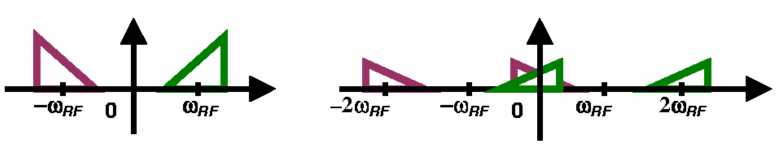

4.2 Spectral Power Densities

LO frame	Rotation by ϕ	Gap frame
$\left(u_{I0}(t), u_{Q0}(t)\right)$	$\rightarrow$	$\left(u_I(t), u_Q(t)\right)$
$\begin{pmatrix} P_{II0}(\omega) & P_{IQ0}(\omega) \\ P_{QI0}(\omega) & P_{QQ0}(\omega) \end{pmatrix}$	$\rightarrow$	$\begin{pmatrix} P_{II}(\omega) & P_{IQ}(\omega) \\ P_{QI}(\omega) & P_{QQ}(\omega) \end{pmatrix}$

Symmetry properties

Main-diagonal spectra

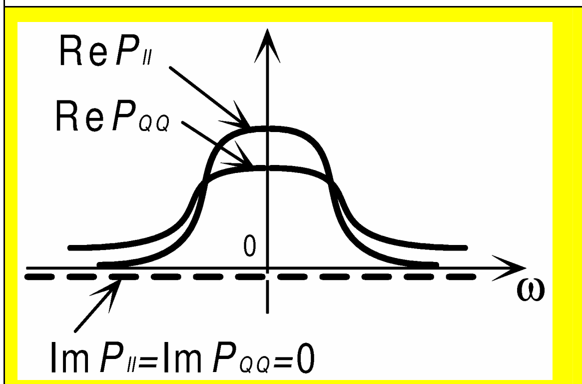

1. Purely real.
2. Non-negative.
3. Even functions of ω.

Off-diagonal spectra

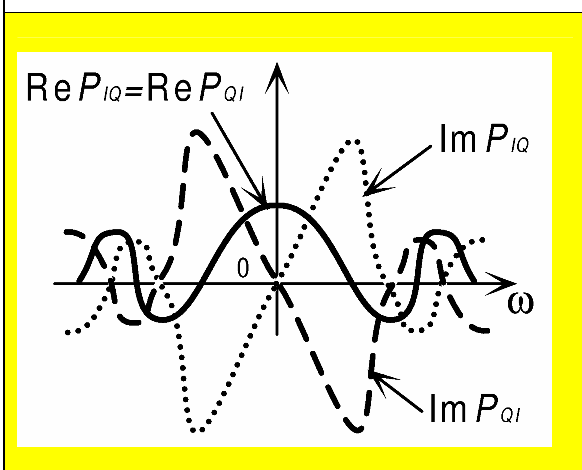

Real parts:

1. Coincident.
2. Even functions of ω.
3. Acquire values >0 and <0.

Imaginary parts:

1. Anti-coincident.
2. Odd functions of ω.

Practical conclusion: to diagnose the **4** real functions:

$$P_{II}(\omega),\ P_{QQ}(\omega),\ \mathrm{Re}\, P_{IQ}(\omega),\ \left\lfloor \mathrm{Im}\, P_{IQ}(\omega) \right\rfloor \text{ in } \omega \geq 0$$

Rotation of Spectra from the LO to gap frames is

$$
\begin{aligned}
&P_{II}(\omega) = P_{II0}(\omega)\cos^2\phi + \operatorname{Re} P_{IQ0}(\omega)\sin 2\phi + P_{QQ0}\sin^2\phi,\\
&P_{QQ}(\omega) = P_{QQ0}(\omega)\cos^2\phi - \operatorname{Re} P_{IQ0}(\omega)\sin 2\phi + P_{II0}\sin^2\phi,\\
&\operatorname{Re} P_{IQ}(\omega) = \operatorname{Re} P_{IQ0}(\omega)\cos 2\phi - \frac{1}{2}\left(P_{II0}(\omega) - P_{QQ0}(\omega)\right)\sin 2\phi,\\
&\operatorname{Im} P_{IQ}(\omega) = \operatorname{Im} P_{IQ0}(\omega).
\end{aligned}
$$

Consequences:

1. Sum $P_{II}(\omega)$ + $P_{QQ}(\omega)$, Im$P_{IQ}(\omega)$ and Im$P_{QI}(\omega)$ are invariants of rotation.
2. Im$P_{IQ}(\omega)$ and Im$P_{QI}(\omega)$ are stand-alone functions having no effect on $P_{II}(\omega)$, $P_{QQ}(\omega)$ or Re$P_{IQ}(\omega)$.

Narrow-banded (n = 0) functions $P_{IQ}(\omega)$ and $P_{QI}(\omega)$ (about the gap frame) would bring about a **trivial** contribution to $D(J)$ in a well $U(\varphi) = U(-\varphi)$

$$
D(J) = \frac{1}{2}\left(\frac{\Omega_0^2}{V_{RF}}\right)^2 \sum_{a,b}\sum_{n,m=-\infty}^{\infty} P_{ab}\left(n\omega_0 + m\Omega_s(J)\right)\cdot V_{mn}^{(a)}(J)V_{mn}^{(b)*}(J)
$$

$$
V_{m0}^{(a)}(J) \neq \begin{cases} 0 & \text{for } m = \text{even} \;\; \& \;\; a = I, \\ 0 & \text{for } m = \text{odd} \;\; \& \;\; a = Q \end{cases}
$$

and = 0 otherwise

3. The non-diagonal spectra $P_{IQ}(\omega)$, $P_{QI}(\omega)$ residual in the gap frame exert no systematic effect on the beam diffusion by themselves

Practical conclusion: to diagnose the **3** real functions:

$$
P_{II}(\omega),\; P_{QQ}(\omega),\; \operatorname{Re} P_{IQ}(\omega) \text{ in } \omega \geq 0
$$

4.3 Noises via 208 or 52 MHz RF systems

Beam bunching — via 208 MHz (mostly).

I/*Q* noise about 208 MHz and/or 52 MHz RF carriers. Which and where is more dangerous?

Weight functions effective in $D(J)$:

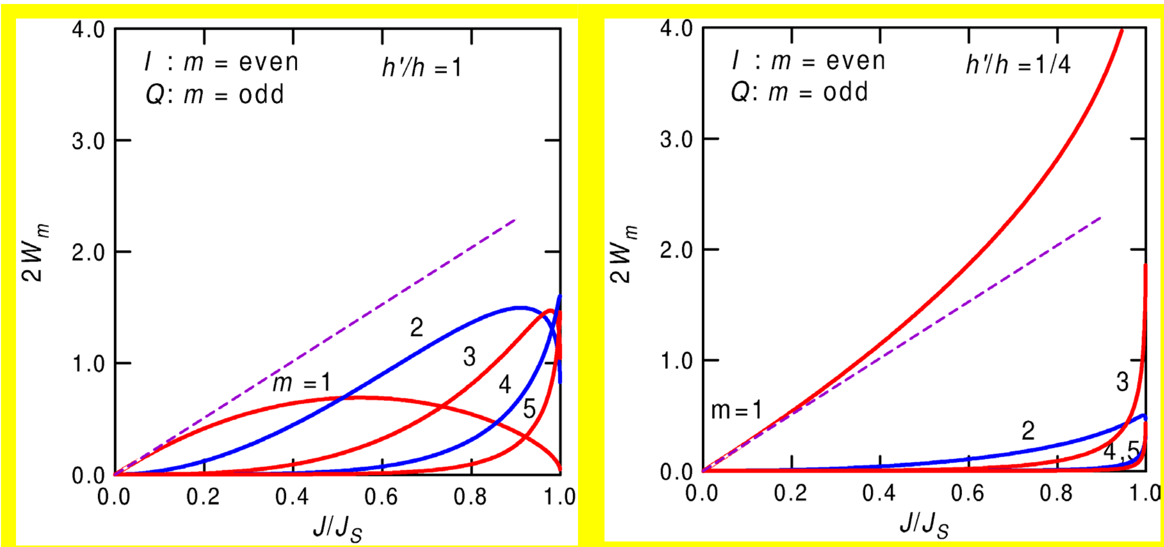

Inside 208 MHz RF bucket, excitation through the 208 MHz harmonic

Inside 208 MHz RF bucket, excitation through the 52 MHz harmonic

Much a poorer non-linear content in case of $h'/h = 1/4$.

The 52 MHz RF sub-harmonic is highly effective in driving the dipole oscillations in an entire range of $J \leq J_S$. Effect increases towards outskirts of a bunch.

Practical conclusion: Noise $P_{QQ}(\omega)$ of the 52 MHz RF system in the dipole side band ($m = \pm 1$) of synchrotron oscillations is much more hazardous inherently than its 208 MHz counterpart. **More attention to 52 MHz RF system!**

4.4 Discrete Fourier Transforms

$$U_a(\omega,T)=\int_{-T/2}^{T/2}u_a(t)\exp(i\omega t)dt$$

Clipping through rectangular-window

$$P_{ab}(\omega_j)=\frac{1}{T}\left\langle U_a(\omega_j,T)\cdot U_b^*(\omega_j,T)\right\rangle$$

@ T >> correlation time of noise

Data record parameters, actual data acquisition

Record length, T	1	s
Time increment, Δt	$2{\cdot}10^{-4}$	s
Sampling rate, R	5000	samples/s
Frequency resolution, $\Delta\omega/2\pi$	1	Hz
Nyquist frequency, $\omega_{Nyq}/2\pi$	2.5	kHz
Observation frequency span	0–250	Hz
Suppression of under-sampled signals towards the monitored 0–250 Hz base-band under a white-noise input	< –10	dB
Size of a record file in the TDS MathCAD format	about 40	kbytes
Dead time between subsequent acquisitions	60–70	s
Number of I & Q samples acquired, S + S	25 + 25	per a session

10 min of CPU-time consumption/per cavity on P3, 1 GHz

<u>Data acquisition control</u>:

Digital scope TEKTRONIX TDS 684A yields

$$M_a(\omega_j)=\frac{1}{T}\left\langle\left|U_a(\omega_j,T)\right|\right\rangle=\frac{1}{T}\left\langle\sqrt{U_a(\omega_j,T)\cdot U_a^*(\omega_j,T)}\right\rangle$$

(300-sweep average with the built-in mathematics)

Control of magnitudes and frequency-domain conduct + consistency of data records

5 Two-Channel Differential Amplifier

5.1 What for?

2 channels — cross-correlation analysis of *I*/*Q* signals

2 inputs per channel — the direct and inverted (differential) ones

The subtraction (differential) technique

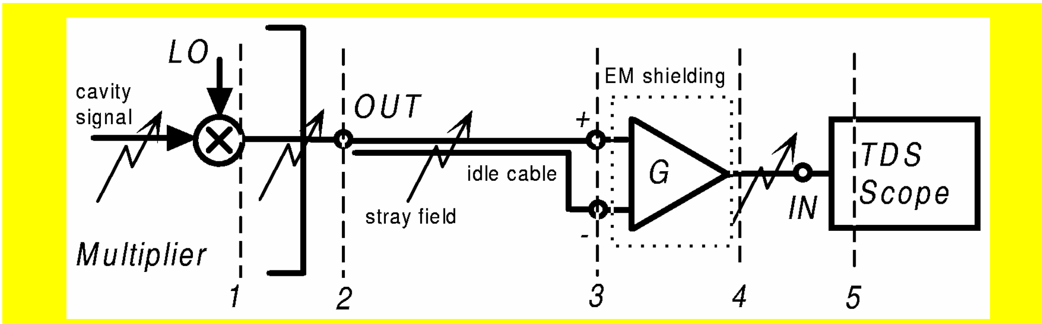

Transfer function of a channel

$$G(\omega) = \pm K \frac{-i\omega}{\omega_L - i\omega} \cdot \frac{\omega_H}{\omega_H - i\omega}$$

The simplest cascade of the passive first-order differentiating and integrating circuits to minimize inherent noise.

Technical specifications

Gain, K (@ RLoad = 1 MOhm)		300	
Lower cut-off frequency, $\omega_L/2\pi$		5	Hz
Higher cut-off frequency $\omega_H/2\pi$		1.1	kHz
Suppression of in-phase signals			
	@ 20 Hz	–70	dB
	@ 1 kHz	–80	dB
Input resistance		20	kOhm
Output resistance		50	Ohm
Long-term drift of DC off-set at output		< ±0.1	mV
AC spurious voltage, peak-to-peak			
	@ output	< ±3	mV
	reduced to the input node	< ±10	μV

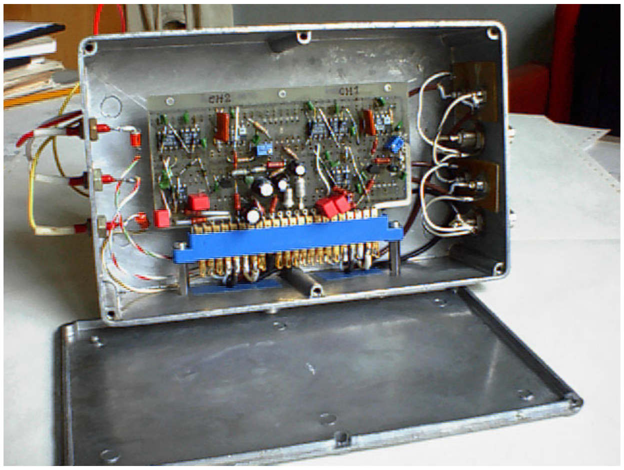

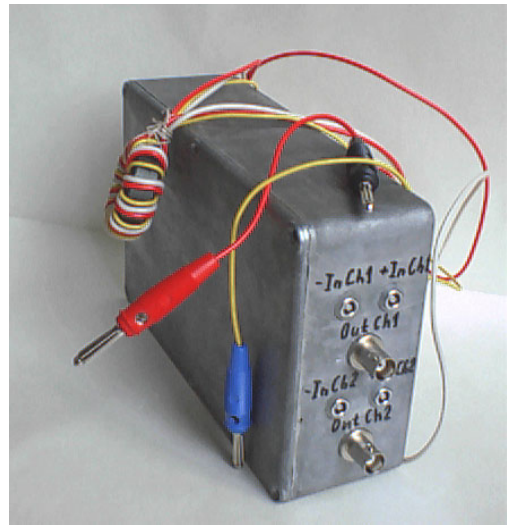

5.2 Performance Data Measurements

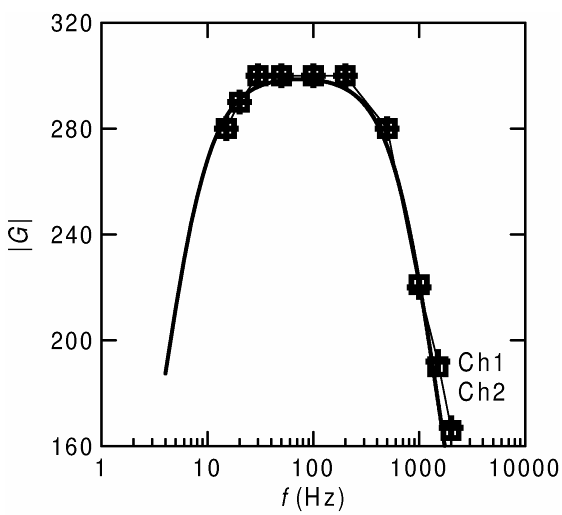

Amplitude-frequency characteristic of the differential amplifier

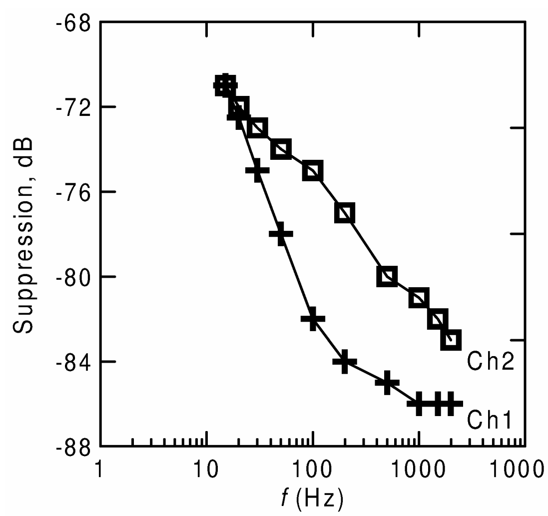

Suppression of a common-mode signal, experimental data points

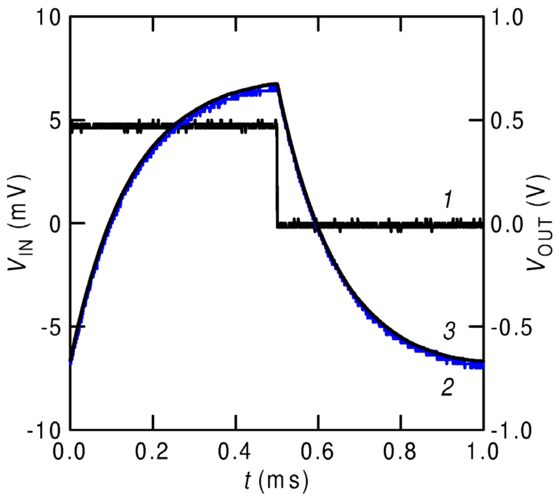

Calibration with the 1 KHz meander

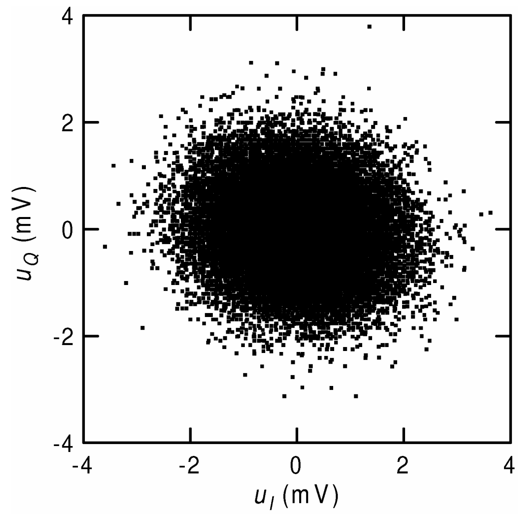

Scatter spot of spurious AC voltages at exit (25 s long observation)

Spot size at 1σ is

±0.90 mV (*I*, channel 1) and ±0.75 mV (*Q*, channel 2)

Since gain K = 300, the value of the self-noise reduced to the entry node is ±(2.5–3.0) μV at 1σ.

5.3 Background & Resolution Threshold

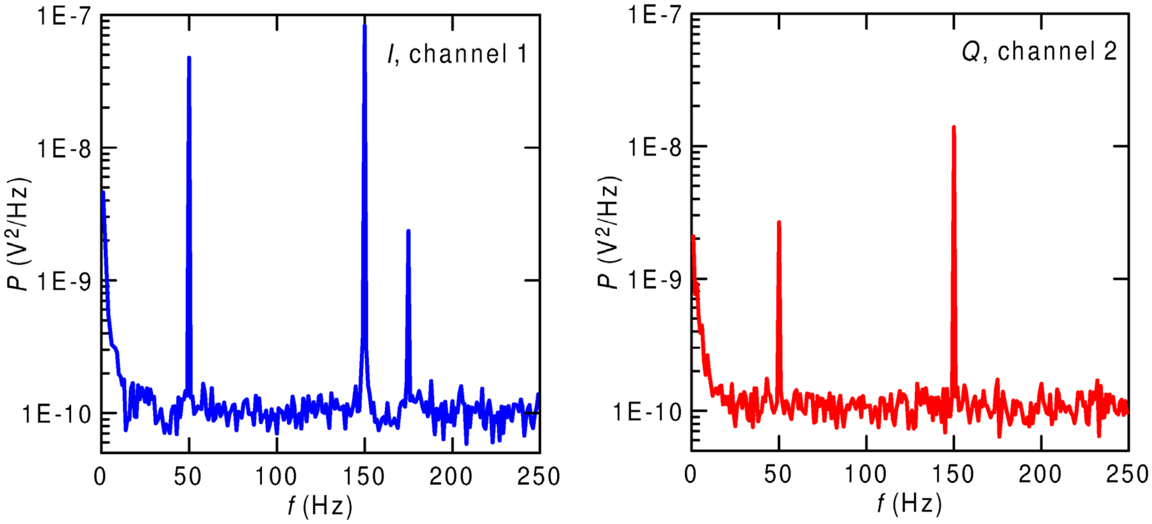

Spectral power densities. Background in channels 1 and 2

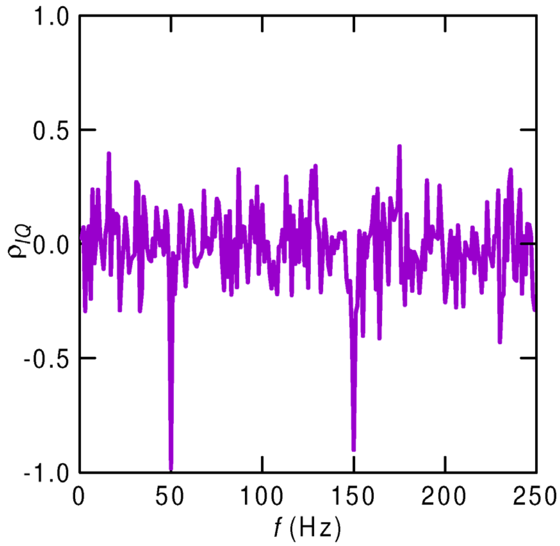

Cross-correlation function of self-noise in channels 1, 2

190 kV → 70 mV in 208 MHz RF system cavity diagnostics

$$P/V_{RF}^2 \cong (1-1.5)\cdot 10^{-10}\,\frac{\mathrm{V}^2}{\mathrm{Hz}}\cdot\frac{1}{(300)^2}\cdot\frac{1}{(70\ \mathrm{mV})^2} \cong (2-3)\cdot 10^{-13}\,\frac{1^2}{\mathrm{Hz}}$$

$$A/V_{RF} \cong \left[\frac{4}{T}(0.02-1)\cdot 10^{-7}\,\frac{\mathrm{V}^2}{\mathrm{Hz}}\cdot\frac{1}{(300)^2}\cdot\frac{1}{(70\ \mathrm{mV})^2}\right]^{1/2} \cong (0.4-3)\cdot 10^{-5}$$

6 Measurements of Noise in RF System

6.1 Generalities

Block diagram of the measuring circuit (208 and/or 52 MHz RF systems)

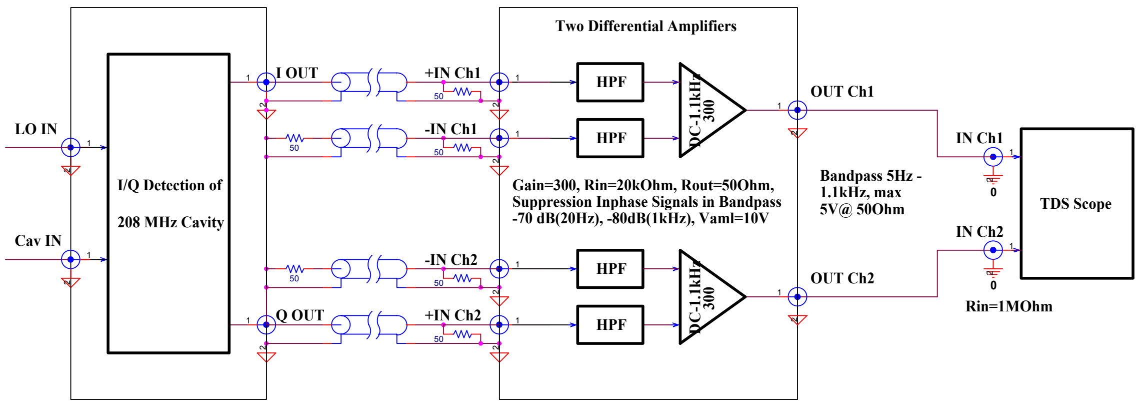

The TDS 684A scope was, basically, employed as a two-channel 8-bit ADC with a capability of converting data records into the MathCad format.

Parameters and a number of the data records must:

1. comply with the higher cut-off in the amplifier,
2. conform to the TDS performance,
3. produce files of a reasonable size,
4. be sufficient to accomplish a reasonable statistical averaging,
5. contain a whole number of 1/50 Hz in record length, and
6. be manageable via PC-based post-processing under a moderate CPU-time consumption.

6.2 Example: cavity A, 208 MHz

As an example, in details …

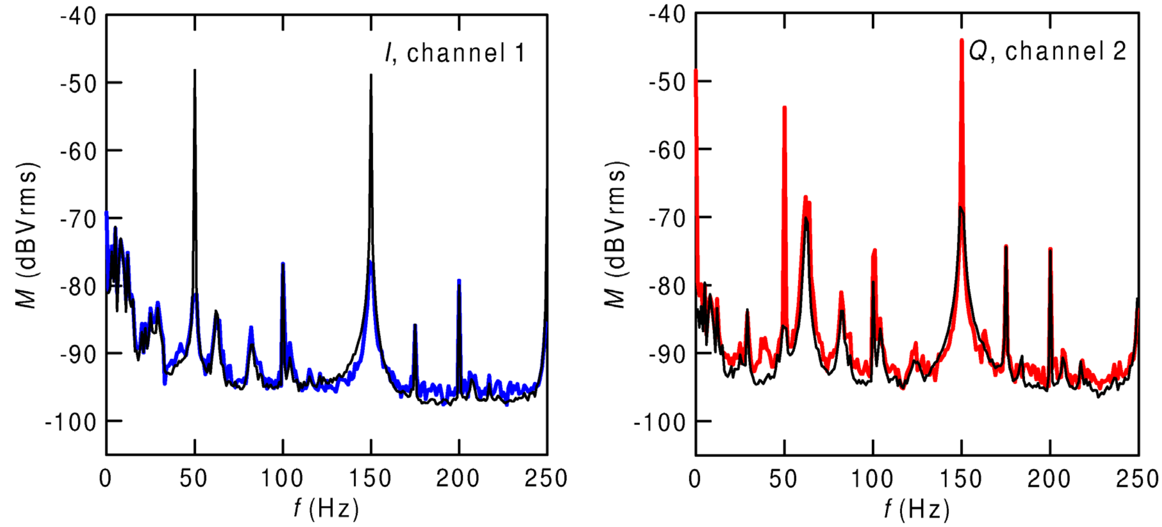

Averaged amplitude of DFT, calculated and directly acquired via the TDS. Cavity A 208 MHz, the LO frame

300 samples by TDS versus 25 samples recorded and processed

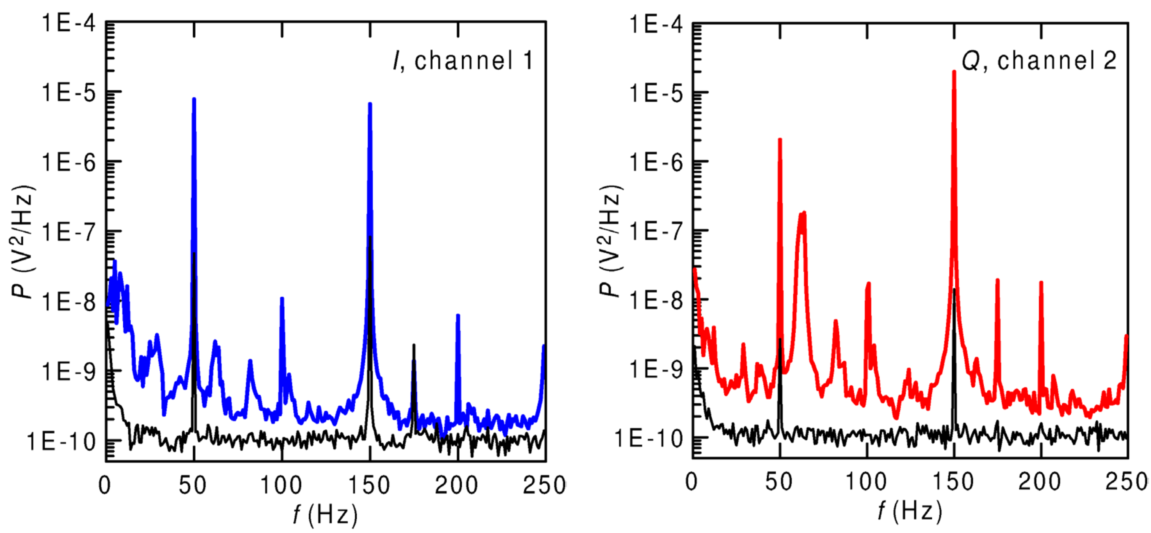

Acquired spectral power densities against resolution threshold (the lower curve). Cavity A 208 MHz, the LO frame

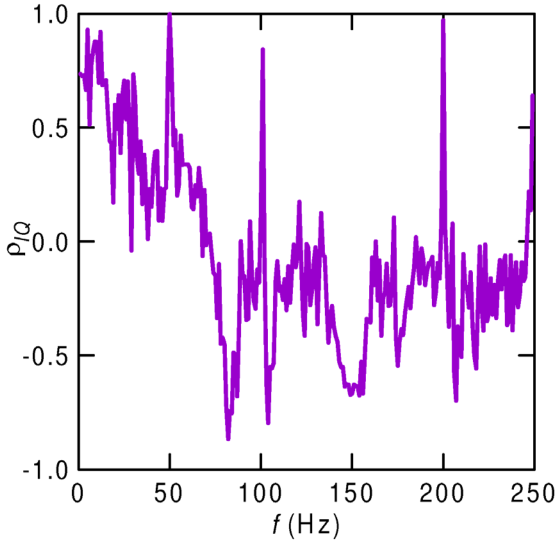

Cross-correlation function of noise. Cavity A 208 MHz, the LO frame

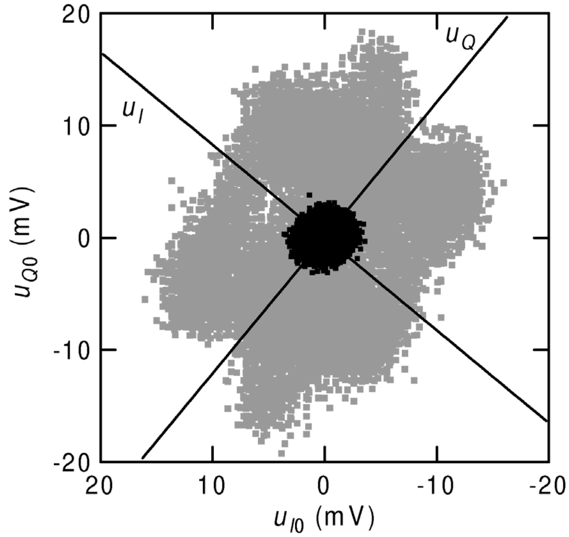

Scatter plot of spurious AC voltages in channels I, Q of the LO frame

Cross-correlation function

$$\rho_{IQ}(\omega) = \frac{\mathrm{Re}\left(P_{IQ}(\omega)\right)}{\sqrt{P_{II}(\omega) P_{QQ}(\omega)}}$$

Further off-line signal processing comprises:

1. Normalization by DC-coupled readout magnitude ($V_{I0}^2 + V_{Q0}^2$) to reduce the spectra to fractional voltage deviations in [1^2/Hz].
2. Rotation by $\phi = \mathrm{atan}(V_{Q0}/V_{I0})$ to move from the LO to gap frame.
3. Multiplication by $1/|G(\omega)|^2$ to correct for the amplitude-frequency distortion caused by the acquisition channel itself.

These options are not available in standard built-in mathematics of any scope!

The final outcome for cavity A 208 MHz:

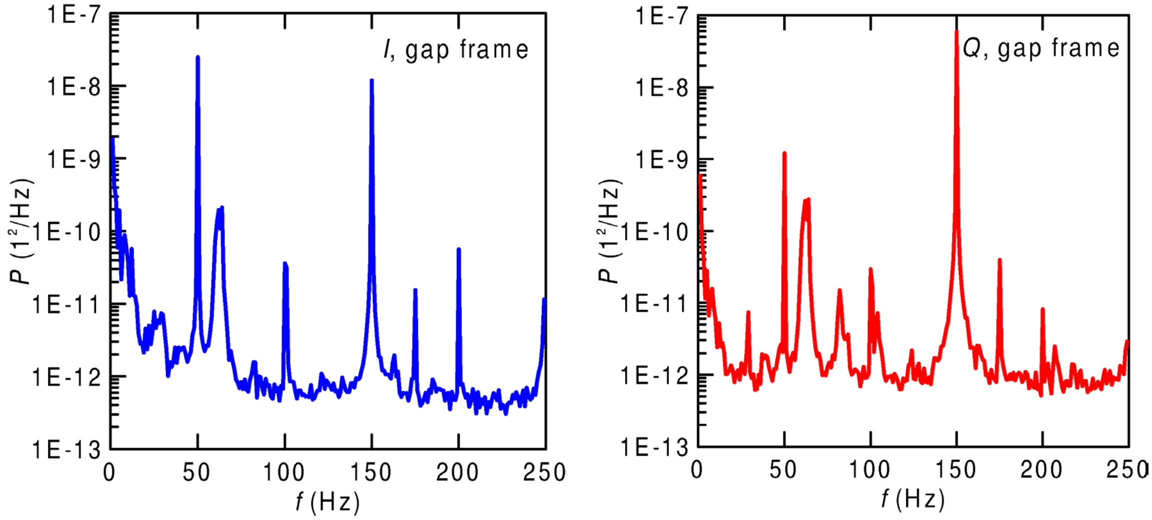

Spectral power densities. Cavity A 208 MHz, the gap frame

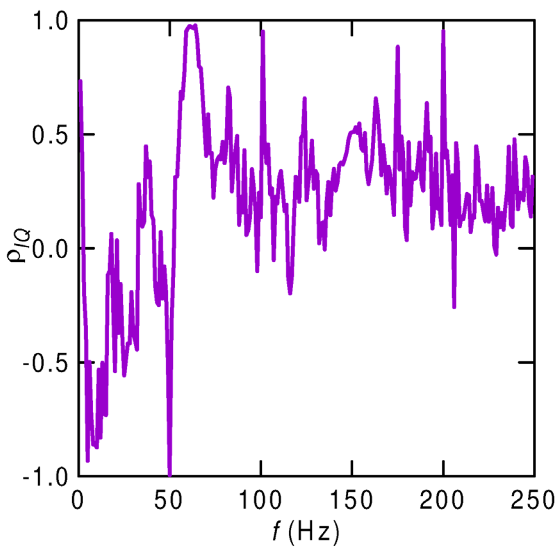

Cross-correlation function of noise. Cavity A 208 MHz, the gap frame

7 Overall Noise Behavior of RF Systems

All together,

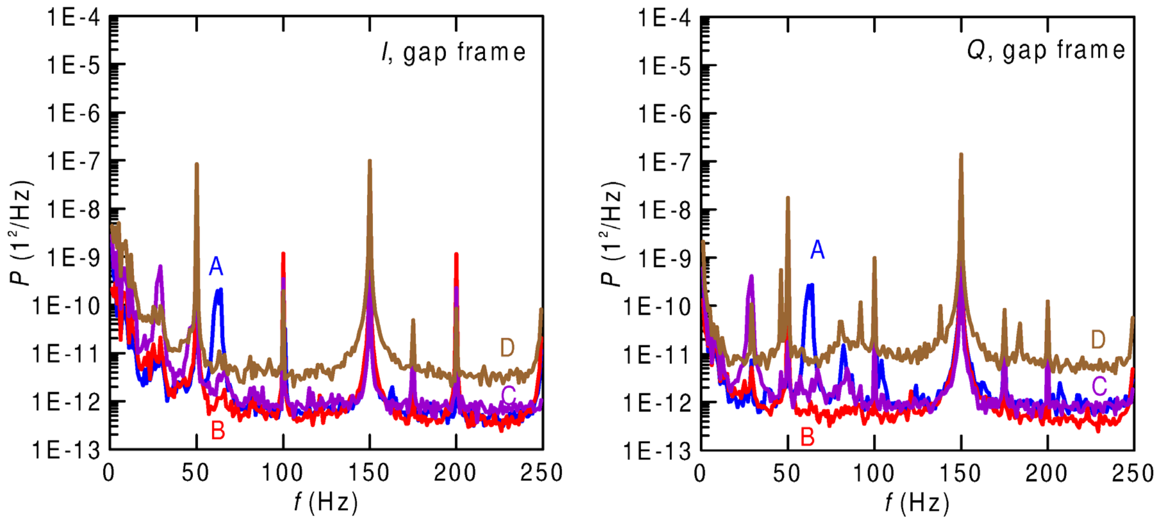

Spectral power densities. Cavities A, B, C and D 208 MHz, the gap frame

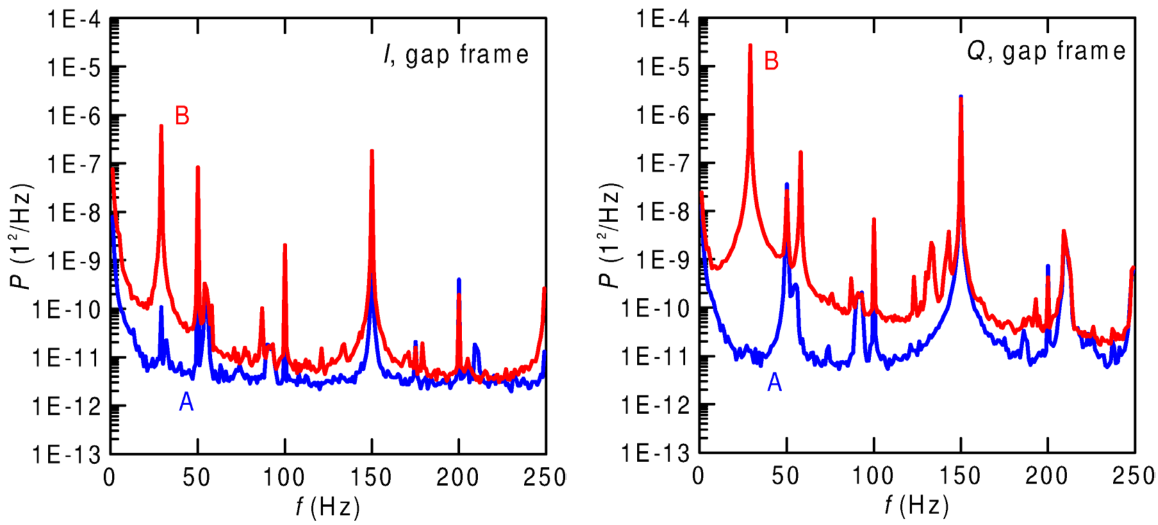

Spectral power densities. Cavities A and B 52 MHz, the gap frame

8 Conclusions

Diagnostic Equipment

1. Use of the purpose-built low-noise base-band amplifiers to follow immediately the down-converting multipliers in the *I*/*Q* modules.

2. Shielding against stray electro-magnetic fields.

3. Use of the subtraction (differential) technique.

Noise Measuring Capability

4. The resolution base-line threshold constitutes a few units of 10^{-13} 1^2/Hz.

5. Alteration of noise behaviour in response to resetting operational parameters of an RF cavity. (A future diagnostic tool for HERA-*p* control system?).

6. In a whole, beam-response observations comply with noise the diagnosed in 208 and 52 MHz RF systems.

Overall Noise Performance of the RF System

7. Level of noises at 208 MHz is lower than it has been expected for. **The 208 MHz RF system shows a satisfactory noise conduct.**

8. Continuous stretch of noise at 52 MHz is noticeably higher.

9. A significant presence of discrete frequency lines in the noise spectra.

10. Amplitude (or *I*) and phase (or *Q*) noises rotated back to the gap frame usually retain a strong residual cross-correlation.

11. **The worst noise performance is proper to cavity B 52 MHz in the lower-frequency band of 10–40 Hz.** The noise spectrum has a pronounced resonant shape.

12. The nature of such a noise is not comprehensible at the moment. Further studies are requested.